12A.2 NUMERICAL SIMULATIONS OF THE HURRICANE INTENSITY RESPONSE TO A WARM OCEAN EDDY

Richard M. Yablonsky* and Isaac Ginis
University of Rhode Island, Narragansett, Rhode Island

1. INTRODUCTION

Hurricanes require evaporative heat flux from the sea surface to intensify and be maintained, and this evaporative heat flux occurs primarily in the storm's core (e.g. Cione and Uhlhorn 2003, Emanuel 2003, and references therein). Since the evaporative heat flux is a function of sea surface temperature (SST), any physical process that alters the storm-core SST may also impact the storm's intensity. In the deep ocean, storm-core SST cooling occurs primarily because the storm's surface winds impose a wind stress on the upper ocean, and the resulting ocean current shear generates turbulent mixing and entrainment of cooler water into the upper oceanic mixed layer (OML) from below (e.g. Ginis 1995, 2002, and references therein). By comparison, evaporative heat flux to the atmosphere has little impact on the storm-core SST (Price 1981; Shen and Ginis 2003; D'Asaro et al. 2007), but for slow-moving hurricanes, upwelling may contribute significantly to storm-core SST cooling (Price 1981; Yablonsky and Ginis 2009, hereafter YG09).

Warm ocean eddies, also known as warm core rings (WCRs), are anticyclonically-rotating upper ocean features that have higher temperatures than their surroundings. In hurricane-prone ocean regions such as the Gulf of Mexico, especially during hurricane season, the horizontal temperature gradient between a WCR and its surroundings may be quite small at the sea surface, but the OML depth is significantly greater in the WCR than in its surroundings, yielding a strong subsurface horizontal temperature gradient and in turn, strong geostrophically-adjusted anticyclonic currents. When a hurricane traverses a WCR, the WCR may impact the hurricane's intensity by altering the storm-core SST cooling.

The most generally accepted mechanism whereby the presence of a WCR can impact storm-core SST cooling is a combination of reduced shear-induced mixing at the base of the OML and the fact that water entrained into the OML from below must be distributed over a greater depth, yielding less cooling at the sea surface. This mechanism is simply a consequence of the increased OML depth in the WCR relative to its surroundings, and it ignores the WCR's anticyclonic circulation. Recently, however, Yablonsky and Ginis (2009a, hereafter YG09a) showed that horizontal advection of the storm's cold wake by a WCR's anticyclonic circulation may impact storm-core SST cooling, especially when the WCR is located to the right of the storm track. Here, the subsequent feedback of an altered storm-core SST cooling on hurricane intensity is investigated using a coupled hurricane-ocean model, with an emphasis on the role of horizontal advection of SST by the WCR's circulation.

* *Corresponding author address:* Richard M. Yablonsky, Univ. of Rhode Island, Graduate School of Oceanography, 215 South Ferry Road, Narragansett, RI 02882; e-mail: ryablonsky@gso.uri.edu.

2. EXPERIMENTAL DESIGN

2.1 *Model Description*

The coupled hurricane-ocean model experiments in this study are performed using a version of the GFDL/URI coupled hurricane-ocean prediction system (hereafter GFDL model) that is similar to the version used operationally at NOAA's National Centers for Environmental Prediction (Bender et al. 2007). The atmospheric component of the model employs the hydrostatic approximation and solves the primitive equations on a longitude-latitude grid with a sigma vertical coordinate. The atmospheric model domain consists of a triply nested grid configuration, in which two inner grids are moveable and two-way interactive. The stationary outermost grid spans 75º by 75º from 110ºW to 35ºW longitude and from 10ºS to 65ºN latitude, with 1/2º grid spacing. The middle grid spans 11º by 11º with 1/6º grid spacing. The innermost grid spans 5º by 5º with 1/12º grid spacing. In the vertical, there are 42 sigma levels. The atmospheric model physics includes a simplified Arakawa and Schubert (1974) scheme for cumulus parameterization (Grell 1993), a Ferrier (2005) cloud microphysics package for large-scale condensation, the Smagorinsky (1963) nonlinear viscosity scheme for horizontal diffusion, the Troen and Mahrt (1986) non-local scheme diffusion for vertical diffusion, the Monin-Obukhov scheme for surface flux calculations with an improved air-sea momentum flux parameterization in strong wind conditions (Kurihara and Tuleya 1974; Moon et al. 2007), the Schwarzkopf and Fels (1991) scheme for infrared radiation, and the Lacis and Hansen (1974) scheme for solar radiation.

The ocean component of the GFDL model is the Princeton Ocean Model (POM; Blumberg and Mellor 1987; Mellor 2004). Here, experiments are performed with both a one-dimensional (1D) and a three-dimensional (3D) version of POM, as in YG09 and YG09a. Only the 3D version of POM (not the 1D version) can account for upwelling and horizontal advection. For all experiments, the ocean grid spans from 108.5ºW to 60ºW longitude and from 10ºN to 47.5°N latitude. Unlike the operational GFDL model, the ocean grid is set on an f-plane, where the earth's rotation rate and the longitudinal grid spacing assume constant latitude of 22.4ºN. There are 508 (449) ocean grid points in the x- (y-) direction, yielding a horizontal grid spacing of 9.8 (9.3) km in the x- (y-) direction. The

entire ocean domain is assumed to be a 2500-m deep ocean (no land or bathymetry), and the 23 half-sigma levels are placed at the following depths: 2.5, 7.5, 12.5, 17.5, 22.5, 27.5, 32.5, 40, 47.5, 55, 67.5, 87.5, 125, 187.5, 275, 387.5, 550, 775, 1050, 1400, 1800, 225, and 2500 m.

Air-sea coupling between the atmospheric and oceanic components of the GFDL model occurs by passing key variables between the two components during time integration. Since the ocean time step is longer than the atmospheric time step, the SST is held constant in the atmospheric model in between ocean time steps. At each ocean time step, the surface wind stress, heat, moisture, and radiative fluxes from the atmospheric component are passed into the ocean component, and the SST from the ocean component (calculated using the atmospheric fluxes from the previous ocean time step) is passed into to the atmospheric component to be used until the next ocean time step.

2.2 *Model Initialization*

The atmosphere is initialized using an idealized, axisymmetric vortex, which is subsequently embedded in a uniform, background environmental wind. The initial vertical profiles of temperature and relative humidity in both the vortex and the environment are specified based on the Global Atlantic Tropical Experiment III conditions, as described in Shen et al (2002). To create the vortex, an uncoupled, axisymmetric version of the atmospheric component of the GFDL model is integrated for 60 h, where the initial vortex is specified and then continuously nudged toward a central pressure, outermost closed isobar, maximum wind speed, radius of maximum winds, and radius of outermost closed isobar of 975 hPa, 1010 hPa, 36 m s-1, 55 km, and 375 km, respectively. After the 60-h axisymmetric model integration, the vortex is placed at (68.0°W, 19.5°N) and embedded in a homogeneous, westward, environmental wind prior to the coupled GFDL model forecast. Coupled model experiments are subsequently performed using environmental wind speeds of 0, 2.5, and 5 m s-1. It should be noted, however, that the hurricane vortex will not translate due westward at the environmental wind speed, primarily because beta drift will add a northwestward component of ~1-2 m s-1 to the storm translation speed (Smith 1993).

In the control experiments (CTRL), the ocean is initialized with a horizontally-homogeneous temperature and salinity profile. These profiles are based on the 0-2500-m portion of the Generalized Digital Environmental Model (GDEM) climatological profile in the Gulf of Mexico Common Water during the month of September (Teague et al. 1990). In the experiments other than CTRL, a WCR is assimilated into the otherwise horizontally-homogeneous ocean of CTRL using the feature-based methodology of Yablonsky and Ginis (2008). This WCR is nearly circular in shape, with a radius of 1.2° (i.e. 133 km along the north-south axis and 123 km along the east-west axis), which is typical of WCRs in the Gulf of Mexico (e.g. Oey et al. 2005). The temperature profile at the center of the WCR is based on the 0-2500-m portion of the September GDEM climatological profile in the Caribbean Sea, except the upper ocean mixed layer temperature, and hence the SST, is adjusted slightly to match the upper ocean mixed layer temperature in the surrounding Gulf Common Water, thereby keeping the SST (but not the subsurface temperature) horizontally-homogeneous in the assimilated field. Next, the 3D ocean model is integrated for 96 hours without wind stress in the vicinity of the WCR, thereby allowing the density and current fields in the WCR to geostrophically adjust. The resulting vertical temperature cross-section is shown in Fig. 1a, and the 87.5-m temperature and sea surface current vector field are shown in Fig. 1b, where the maximum sea surface current velocity in the geostrophically-adjusted WCR is ~1.2 m s^{-1}. This ocean temperature field is then used to initialize both the 1D and 3D coupled model experiments, but the WCR's geostrophic currents are removed for the 1D experiments. During coupled model integration, which continues for 120-h, the hurricane translates westward and northward towards and then past a WCR (except in CTRL, where no WCR is present). This WCR is strategically placed so that experiments can be performed with the WCR located in the center of the storm track (WCRC), to the left of the storm track (WCRL), and to the right of the storm track (WCRR), with the center of the storm passing in closest proximity to the center of the WCR ~96-h into model integration (Figs. 2, 3, and 4). Table 1 summarizes the important parameters for all coupled model experiments.

TABLE 1. Important parameters for all experiments.

Experiment Name	Ring Location	Environmental Wind (m s^{-1})	Ocean Model Dimensions
CTRL-0.0-3D	None	0.0	3D
CTRL-0.0-1D	None	0.0	1D
CTRL-2.5-3D	None	2.5	3D
CTRL-2.5-1D	None	2.5	1D
CTRL-5.0-3D	None	5.0	3D
CTRL-5.0-1D	None	5.0	1D
WCRC-0.0-3D	Center	0.0	3D
WCRC-0.0-1D	Center	0.0	1D
WCRC-2.5-3D	Center	2.5	3D
WCRC-2.5-1D	Center	2.5	1D
WCRC-5.0-3D	Center	5.0	3D
WCRC-5.0-1D	Center	5.0	1D
WCRL-0.0-3D	Left	0.0	3D
WCRL-0.0-1D	Left	0.0	1D
WCRL-2.5-3D	Left	2.5	3D
WCRL-2.5-1D	Left	2.5	1D
WCRL-5.0-3D	Left	5.0	3D
WCRL-5.0-1D	Left	5.0	1D
WCRR-0.0-3D	Right	0.0	3D
WCRR-0.0-1D	Right	0.0	1D
WCRR-2.5-3D	Right	2.5	3D
WCRR-2.5-1D	Right	2.5	1D
WCRR-5.0-3D	Right	5.0	3D
WCRR-5.0-1D	Right	5.0	1D

3. RESULTS AND DISCUSSION

Before analyzing the hurricane intensity, it is instructive to first examine the average SST cooling within the storm core, defined here to be within a 60-km radius (dSST-60), as in Cione and Uhlhorn (2003), YG09, and YG09a. The dSST-60 during the hurricane's passage by the WCR (hours 72-120) for all experiments is shown in Figs. 5, 6, and 7. Unlike the uncoupled ocean model experiments with prescribed wind forcing presented in YG09 and YG09a, dSST-60 varies over time in the CTRL experiments, especially for CTRL-0.0-3D (Fig. 5b), in which subtle differences in storm translation speed may have a significant impact on the location and magnitude of upwelling and subsequent contribution of upwelling to both dSST-60 and storm intensity. In addition, storm intensity and structure are changing in the coupled model in response to the SST cooling. Regardless, the CTRL dSST-60 provides a suitable baseline for measuring the impact of a WCR in each of the non-CTRL experiments.

Consistent with YG09a, passage of the storm over the WCR in the WCRC experiments decreases the magnitude of dSST-60 relative to the CTRL experiments in both the 1D experiments (Figs. 5a, 6a, and 7a) and the 3D experiments (Figs. 5b, 6b, and 7b). Also consistent with YG09a, the magnitude of WCRR-1D dSST-60 generally decreases at least slightly relative to CTRL-1D dSST-60 as the storm passes the WCR (Figs. 5a, 6a, and 7a), but the magnitude of the WCRR-3D dSST-60 generally increases relative to CTRL-3D dSST-60 (except in the 5.0 m s^{-1} experiment) as the storm passes the WCR (Figs. 5b, 6b, and 7b). This increase in the magnitude of the WCRR-3D dSST-60 relative to CTRL-3D dSST-60 is likely caused by the WCR's anticyclonic circulation, which advects the storm's cold wake horizontally in the direction of the storm track, thereby increasing the SST cooling underneath the storm core. The results for WCRL are more subtle and less conclusive, but at least for the 0.0 m s^{-1} experiments, the magnitude of WCRL-0.0-3D dSST-60 (Fig. 5b) decreases to a greater extent than the WCRL-0.0-1D dSST-60 (Fig. 5a) as the storm passes the WCR, suggesting that the WCR's circulation advects the storm's cold wake further behind the storm. Returning to the 3D dSST-60, it is also interesting to note that particularly in the 2.5 m s^{-1} experiments (Fig. 6b), the presence of a WCR (regardless of location relative to the storm track) decreases the magnitude of dSST-60 relative to CTRL well before the storm reaches the WCR (i.e. forecast hour 78); this result may be due to either reduced mixing or horizontal advection ahead of the storm center.

The central pressure during the hurricane's passage by the WCR is shown for all experiments in Figs. 8, 9, and 10. In the 1D experiments (Figs. 8a, 9a, and 10a), the only clear and consistent trend is a decrease in the central pressure in the WCRC experiments relative to CTRL as the storm traverses the WCR, suggesting that the reduction in SST cooling due to the presence of a thicker OML allows the storm to intensify in the presence of a WCR. In the 3D experiments (Figs. 8b, 9b, and 10b), the central pressure also decreases in the WCRC experiments relative to CTRL as the storm traverses the WCR, but the difference is significantly larger between WCRC-0.0-3D and CTRL-0.0-3D (Fig. 8b), up to ~15 hPa, than between WCRC-0.0-1D and CTRL-0.0-1D (Fig. 8a), up to ~10 hPa, highlighting the impact of upwelling in the 0.0 m s^{-1} experiments. Even irrespective of the WCR experiments, the fact that the central pressure is ~5-15 hPa lower in CTRL-0.0-1D (Fig. 8a) than in CTRL-0.0-3D (Fig. 8b) suggests that upwelling plays a significant role in weakening the storm in CTRL-0.0-3D.

For this study, however, the focus is on the impact of advection in the WCRR and perhaps WCRL experiments. Interestingly, the difference in central pressure in the 3D experiments (Figs. 8b, 9b, and 10b) between WCRR and CTRL is generally small, even for the 0.0 m s^{-1} experiments (Fig. 8b). In the 3D 0.0 m s^{-1} and 2.5 m s^{-1} experiments (Figs. 8b and 9b), however, the fact that WCRL has a significantly lower central pressure than both WCRR and CTRL (even if not as low as WCRC) as the storm traverses the WCR indicates that advection plays a non-negligible role unless the storm is moving quickly, as in the 3D 5.0 m s^{-1} experiments (Fig. 10b). Returning to the 3D 2.5 m s^{-1} experiments (Fig. 9b), it is particularly helpful to examine the central pressure trend after forecast hour 93. While the central pressure remains nearly constant in CTRL and WCRL, and it decreases, as expected, in WCRC, the central pressure in WCRR increases by ~5 hPa in 9 h between forecast hours 93 and 102. This pressure trend provides rather strong support for the impact of cold wake advection on storm intensity in the WCRR-2.5-3D experiment. Finally, it should be noted that the presence of a WCR (regardless of location relative to the storm track) decreases the central pressure relative to CTRL well before the storm reaches the WCR in the 3D 2.5 m s^{-1} experiments (Fig. 9b), consistent with the dSST-60 change discussed previously and shown in Fig. 6b.

4. SUMMARY AND CONCLUSIONS

The anticyclonic circulation around the periphery of a WCR can advect a hurricane's cold wake towards (away) from the storm core when the WCR is located to the right (left) of the storm track. Qualitatively, the storm-core SST cooling results presented here using a coupled hurricane-ocean model are consistent with YG09a's uncoupled ocean model results using a prescribed wind stress, in that storm-core SST cooling increases (decreases) as the storm passes a WCR when the WCR is located to the right (left) of the storm track. Storm intensity, measured using the storm's central pressure as the key parameter, is also sensitive to the location of the WCR relative to the storm track. Using the experiment with a 2.5 m s^{-1} steering wind and 3D ocean coupling as an example, the presence of a WCR (regardless of location relative to the storm track) first causes the storm to intensify as the storm approaches the WCR, but then as the storm traverses

the WCR, the hurricane continues to intensify (remains nearly steady) (weakens by ~5 hPa) if the WCR is located in the center (to the left) (to the right) of the storm track. The weakening in the latter case is clearly associated with the increased storm-core SST cooling due to advection of the hurricane's cold wake by the anticyclonic circulation around the periphery of the WCR. In the experiments with 1D coupling, however, in which advection is neglected, there are no clear and consistent differences in the intensity change when the WCR is located to the left of the storm track versus to the right of the storm track. This result underscores the limitations of 1D ocean coupling when attempting to model hurricane intensity change during the interaction between a hurricane and a WCR.

The results presented here provide evidence for the impact of a WCR on hurricane intensity and in particular, for the role of horizontal advection due to the WCR's anticyclonic circulation when the WCR is located to the left or right of the storm track. However, the connection between storm-core SST change and subsequent hurricane intensity change is not consistently one-to-one, so it might be worthwhile to explore this connection in more detail. To begin this task, a thorough investigation of the ocean temperature and currents, as in YG09 and YG09a, may be required, and it would also be helpful to examine changes in the storm's size and structure over time and to adjust the definition of the storm-core SST accordingly, as well as to examine the magnitude and spatial distribution of air-sea heat and perhaps momentum fluxes. Such an investigation is beyond the scope of this study, but it could form the basis for future work.

5. REFERENCES

Arakawa, A., and W. H. Schubert, 1974: Interaction of a cumulus cloud ensemble with the large-scale environment, Part I. J. Atmos. Sci., 31, 674-701.

Bender, M. A., I. Ginis, R. Tuleya, B. Thomas, and T. Marchok, 2007: The operational GFDL Coupled Hurricane-Ocean Prediction System and a summary of its performance. Mon. Wea. Rev., 135, 3965-3989.

Blumberg, A. F., and G. L. Mellor, 1987: A description of a three-dimensional coastal ocean circulation model. Three-Dimensional Coastal Ocean Models. N. Heaps, Ed., Vol. 4, Amer. Geophys. Union, 1-16.

Cione, J. J., and E. W. Uhlhorn, 2003: Sea surface temperature variability in hurricanes: Implications with respect to intensity change. Mon. Wea. Rev., 131, 1783-1796.

D'Asaro, E. A., T. B. Sanford, P. P. Niiler, and E. J. Terrill, 2007: Cold wake of Hurricane Frances. Geophys. Res. Lett., 34, L15609, doi:10.1029/2007GL030160.

Emanuel, K., 2003: Tropical cyclones. Ann. Rev. Earth Planet. Sci., 31, 75-104.

Ferrier, B. S., 2005: An efficient mixed-phase cloud and precipitation scheme for use in operational NWP models. EOS, Trans. Amer. Geophys. Union, 86, Jt. Assem. Suppl., Abstract A42A-02.

Ginis I., 1995: Interaction of tropical cyclones with the ocean. Global Perspectives on Tropical Cyclones, Ch. 5, R. L. Elsberry, Ed., Tech. Doc. WMO/TD No. 693, World Meteorological Organization, Geneva, Switzerland, 198-260.

Ginis, I., 2002: Tropical cyclone-ocean interactions. Atmosphere-Ocean Interactions, Advances in Fluid Mechanics Series, No. 33, WIT Press, 83-114.

Grell, G. A., 1993: Prognostic evaluation of assumptions used by cumulus parameterizations. Mon. Wea. Rev., 121, 764-787.

Kurihara, Y., and R. E. Tuleya, 1974: Structure of a tropical cyclone developed in a three-dimensional numerical simulation model. J. Atmos. Sci., 31, 893-919.

Lacis, A. A., and J. Hansen, 1974: A parameterization for the absorption of solar radiation in the earth's atmosphere. J. Atmos. Sci., 31, 118-133.

Leipper, D., and D. Volgenau, 1972: Hurricane heat potential of the Gulf of Mexico. J. Phys. Oceanogr., 2, 218–224.

Mellor, G. L., 2004: Users guide for a three-dimensional, primitive equation, numerical ocean model (June 2004 version). Prog. in Atmos. and Ocean. Sci, Princeton University, 56 pp.

Moon, I.-J., I. Ginis, T. Hara, and B. Thomas, 2007: A physics-based parameterization of air-sea momentum flux at high wind speeds and its impact on hurricane intensity predictions. Mon. Wea. Rev., 135, 2869-2878.

Oey, L.-Y., T. Ezer, and H.-C. Lee, 2005: Loop Current, rings, and related circulation in the Gulf of Mexico: A review of numerical models and future challenges. Circulation in the Gulf of Mexico: Observations and Models, Geophys. Monogr., Vol. 161, Amer. Geophys. Union, 31-56.

Price, J., 1981: Upper ocean response to a hurricane. J. Phys. Oceanogr., 11, 153-175.

Schwarzkopf, M. D., and S. B. Fels, 1991: The simplified exchange method revisited: An accurate, rapid method for computation of infrared cooling rates and fluxes. J. Geophys. Res., 96, 9075-9096.

Shen, W., and I. Ginis, 2003: Effects of surface heat flux-induced sea surface temperature changes on tropical cyclone intensity. Geophys. Res. Lett., 30, 1933, doi:10.1029/2003GL017878.

Shen, W., I. Ginis, and R. E. Tuleya, 2002: A numerical investigation of land surface water on landfalling hurricanes. J. Atmos. Sci., 59, 789-802.

Smagorinsky, J., 1963: General circulation experiments with the primitive equations. Mon. Wea. Rev., 91, 99-164.

Smith, R. B., 1993: A hurricane beta-drift law. J. Atmos. Sci., 50, 3213-3215.

Teague, W. J, M. J. Carron, and P. J. Hogan, 1990: A comparison between the Generalized Digital Environmental Model and Levitus climatologies. J. Geophys. Res., 95, 7167-7183.

Troen, I. B., and L. Mahrt, 1986: A simple model of the atmospheric boundary layer; sensitivity to surface evaporation. Bound.-Layer Meteor., 37, 129-148.

Yablonsky, R. M., and I. Ginis, 2008: Improving the ocean initialization of coupled hurricane-ocean models using feature-based data assimilation. Mon. Wea. Rev., 136, 2592-2607.

Yablonsky, R. M., and I. Ginis, 2009: Limitation of one-dimensional ocean models for coupled hurricane-ocean model forecasts. Mon. Wea. Rev., 137, 4410-4419.

Yablonsky, R. M., and I. Ginis, 2009a: Impact of a warm ocean eddy's circulation on hurricane-induced sea surface cooling with implications for hurricane intensity. Preprints, *16th Conf. on Air-Sea Interaction,* Phoenix, AZ, Amer. Meteor. Soc., 6A.4.

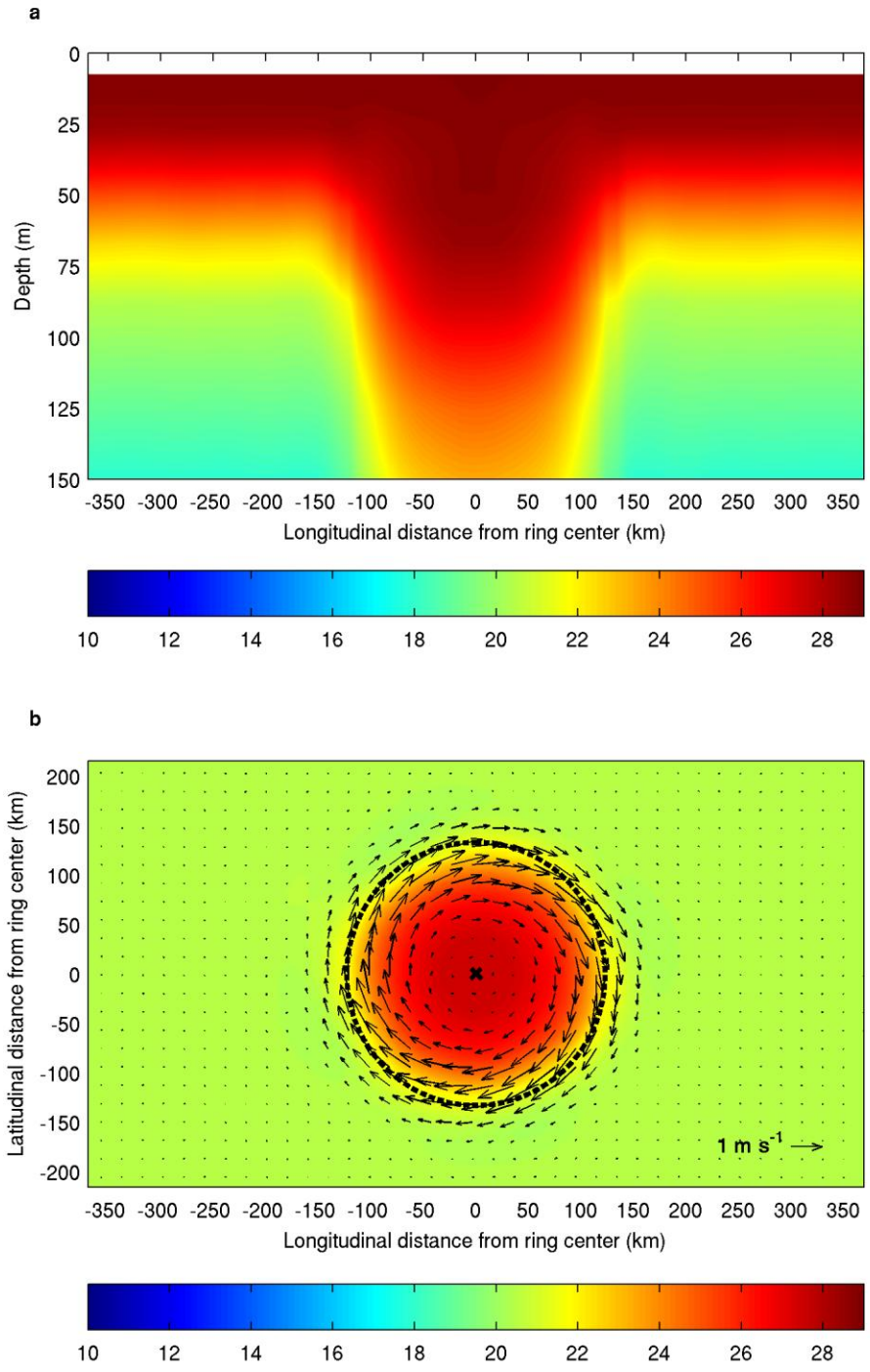

FIG. 1. (a) Ocean temperature (°C) cross-section through the undisturbed WCR and (b) 87.5-m temperature (°C) and sea surface current vectors (3D simulations only) in and around the undisturbed WCR; the WCR's perimeter is indicated by the dashed circle, the WCR's center is indicated by the "x" marker, and the 1 m s^{-1} current vector scale is shown in the lower-right.

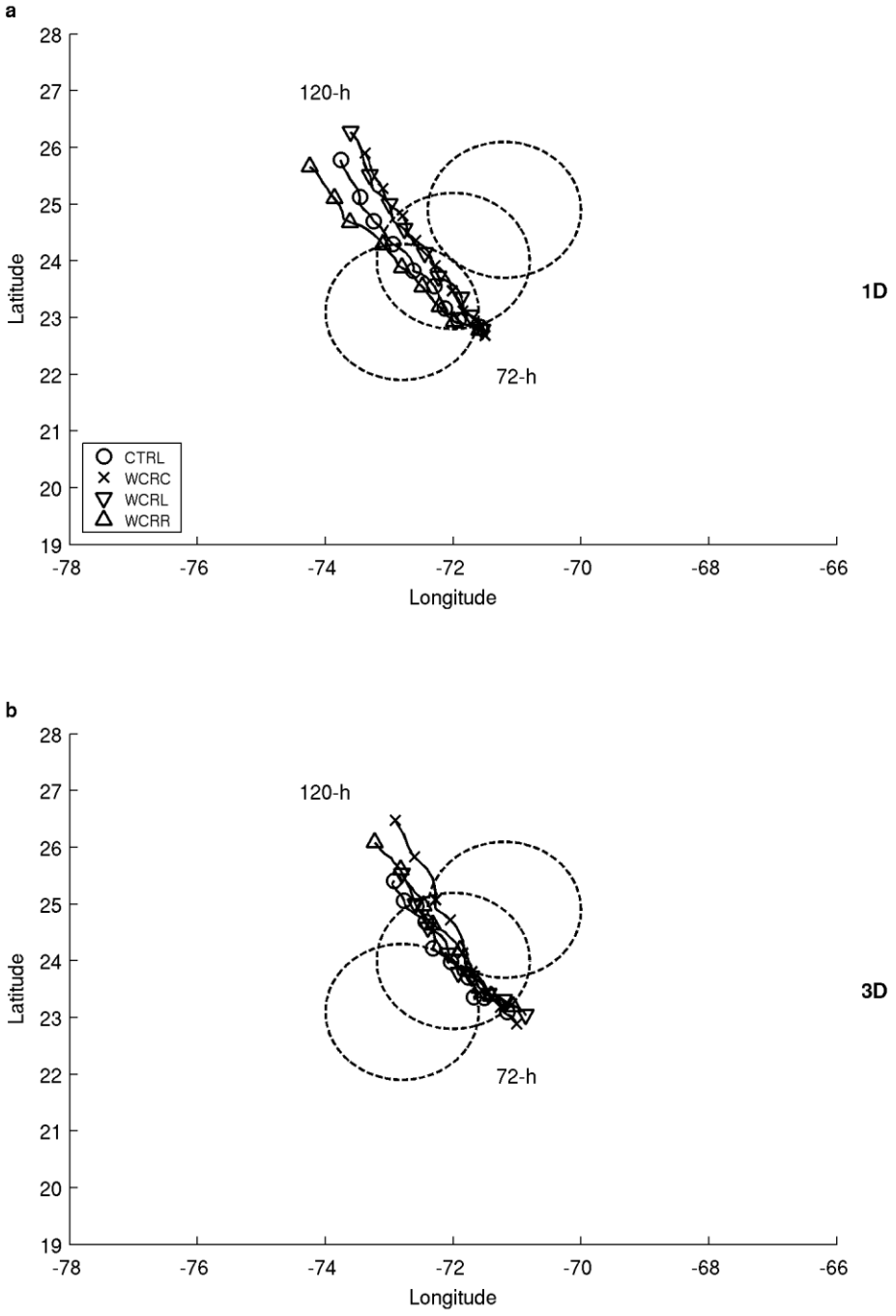

FIG. 2. Storm tracks for hours 72-120 of the CTRL (“o”), WCRC (“x”), WCRL (downward triangle), and WCRR (upward triangle) coupled model simulations with an environmental wind speed of 0.0 m s^{-1} and ocean model dimensions of (a) 1D and (b) 3D. Dashed rings indicate the position of the WCR, with WCRC (WCRL) (WCRR) near the center (left edge) (right edge) of the storm track.

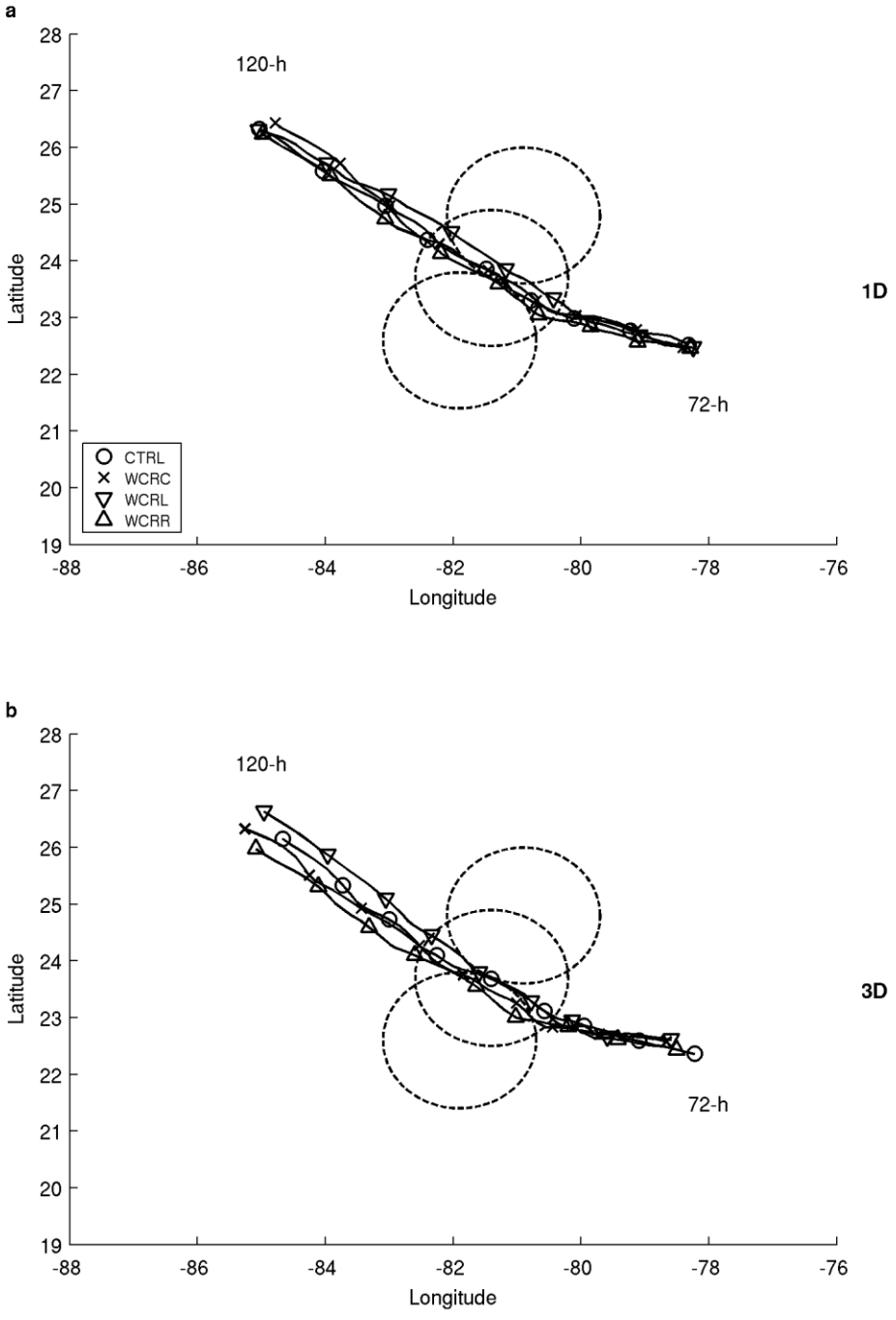

FIG. 3. Same as Fig. 2 but with an environmental wind speed of 2.5 m s^{-1}.

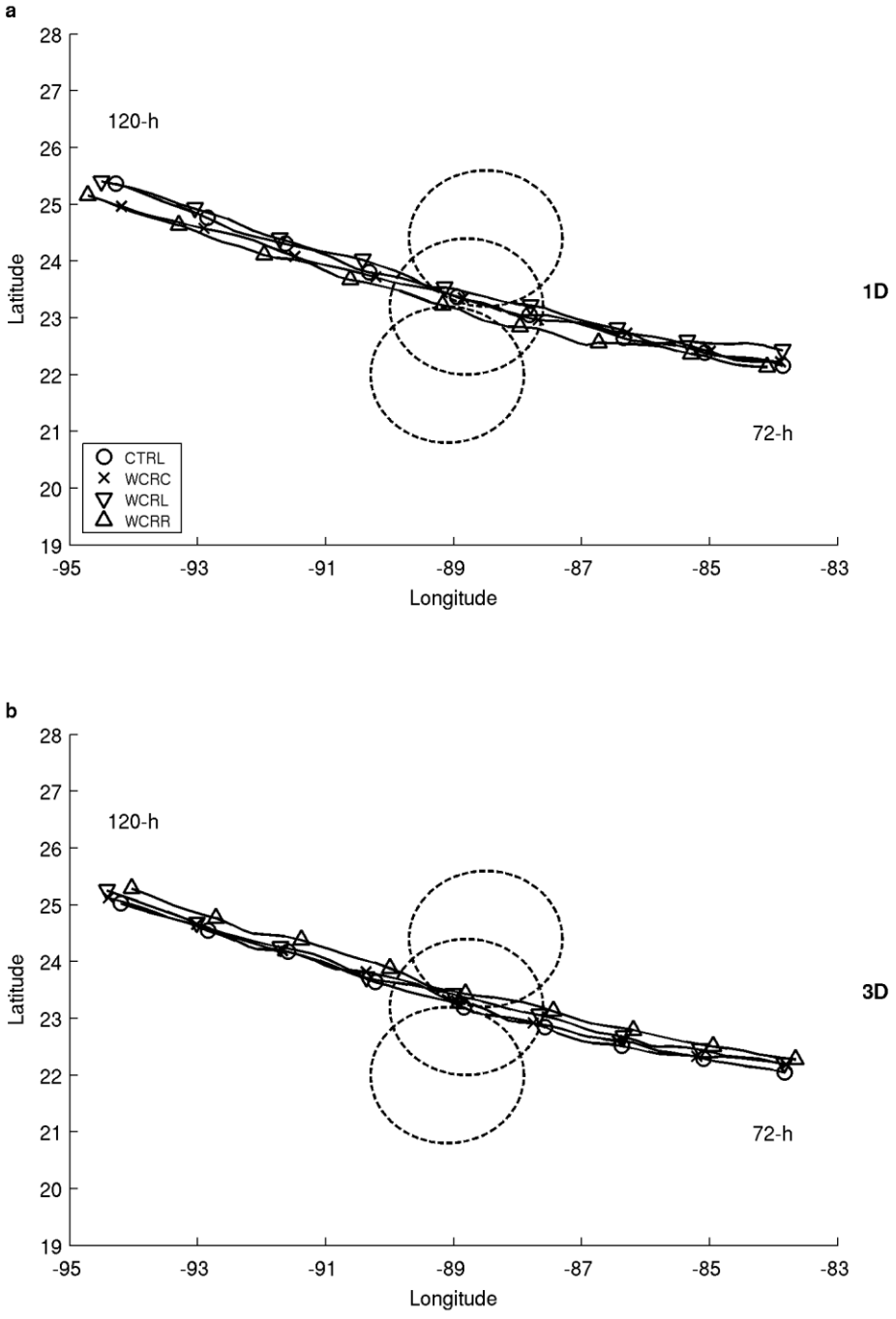

FIG. 4. Same as Fig. 2 but with an environmental wind speed of 5.0 m s^{-1}.

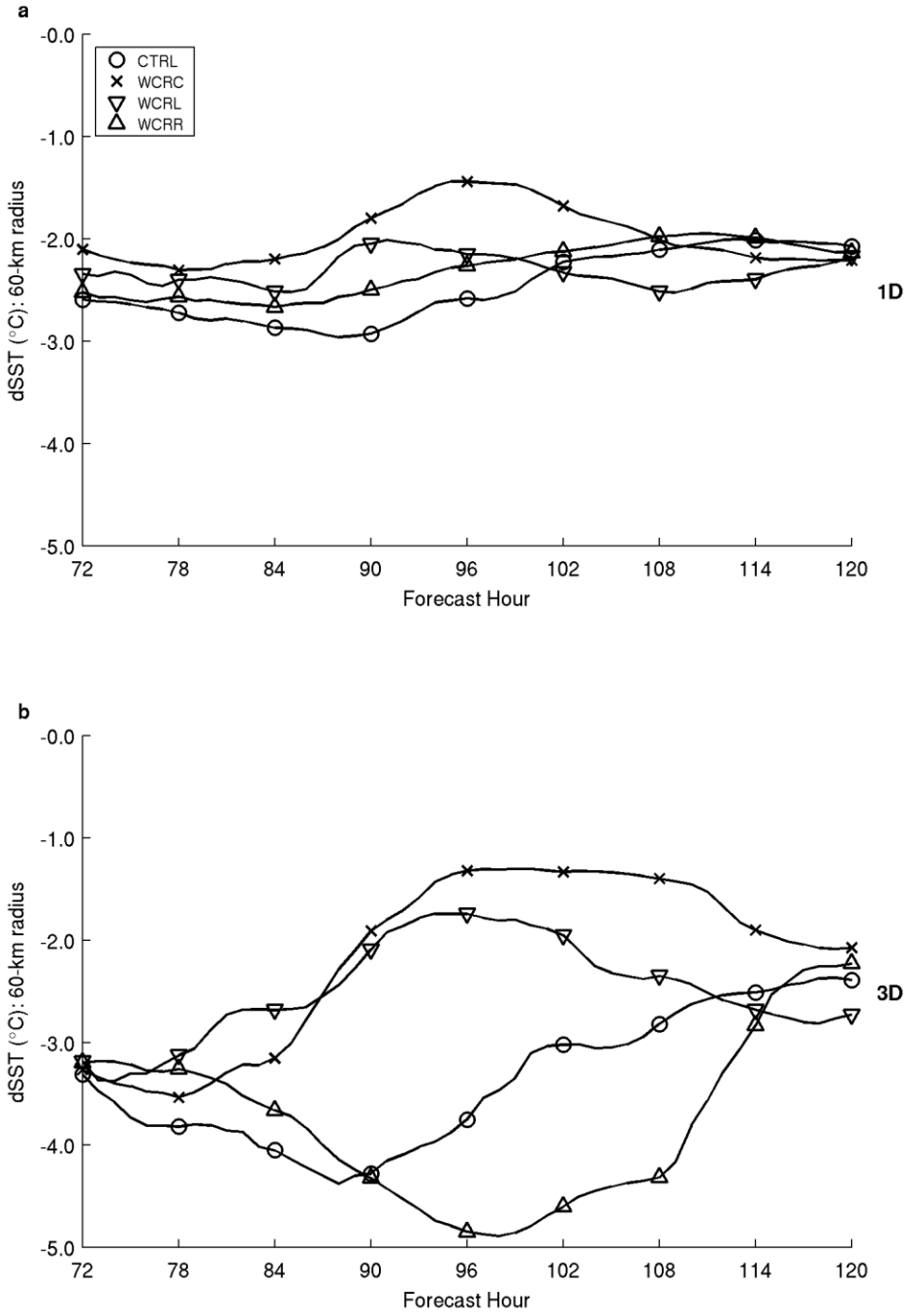

FIG. 5. Average SST cooling within a 60-km radius of the storm center (dSST-60) for hours 72-120 of the CTRL (“o”), WCRC (“x”), WCRL (downward triangle), and WCRR (upward triangle) coupled model simulations with an environmental wind speed of 0.0 m s^{-1} and ocean model dimensions of (a) 1D and (b) 3D.

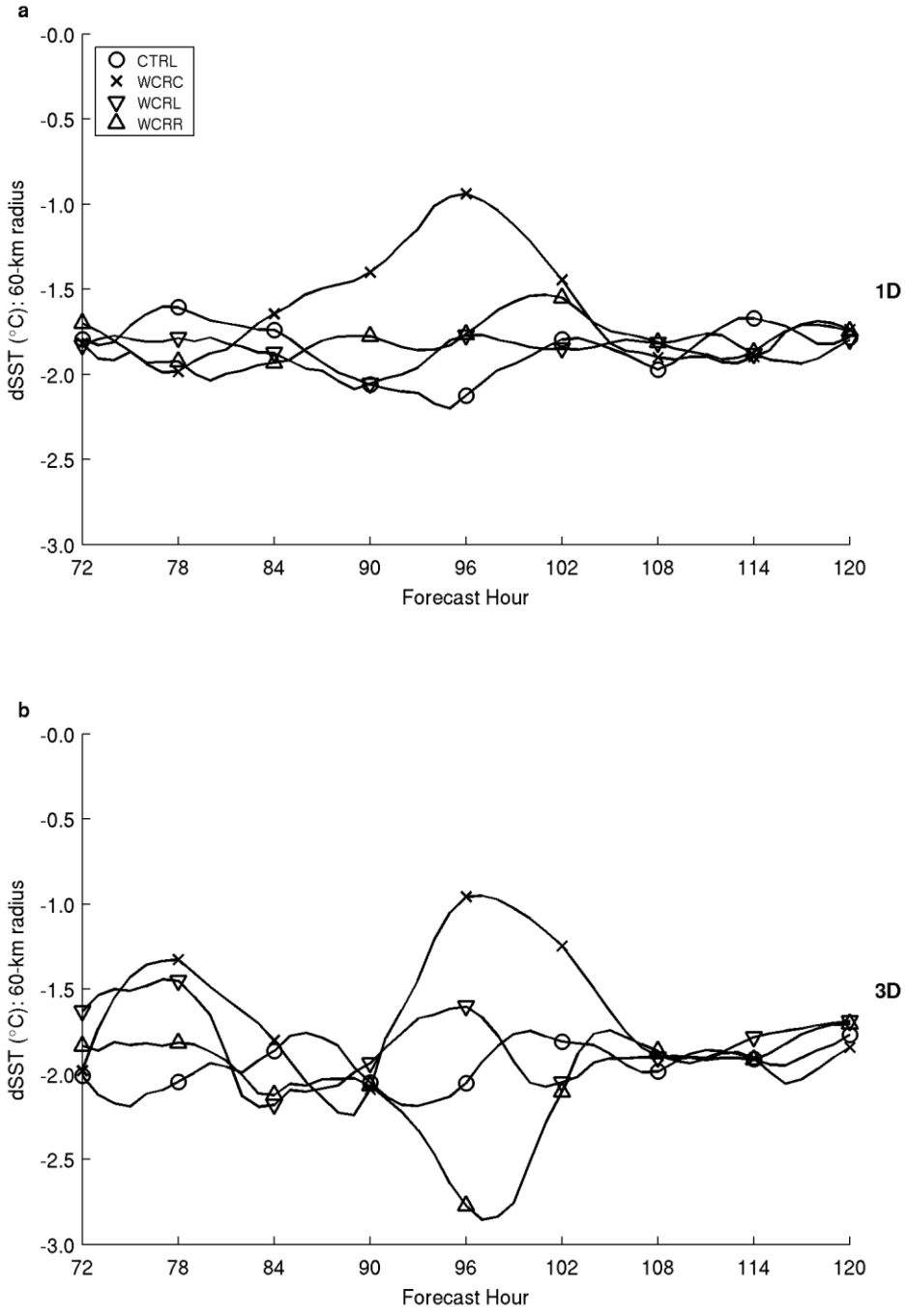

FIG. 6. Same as Fig. 5 but with an environmental wind speed of 2.5 m s^{-1}.

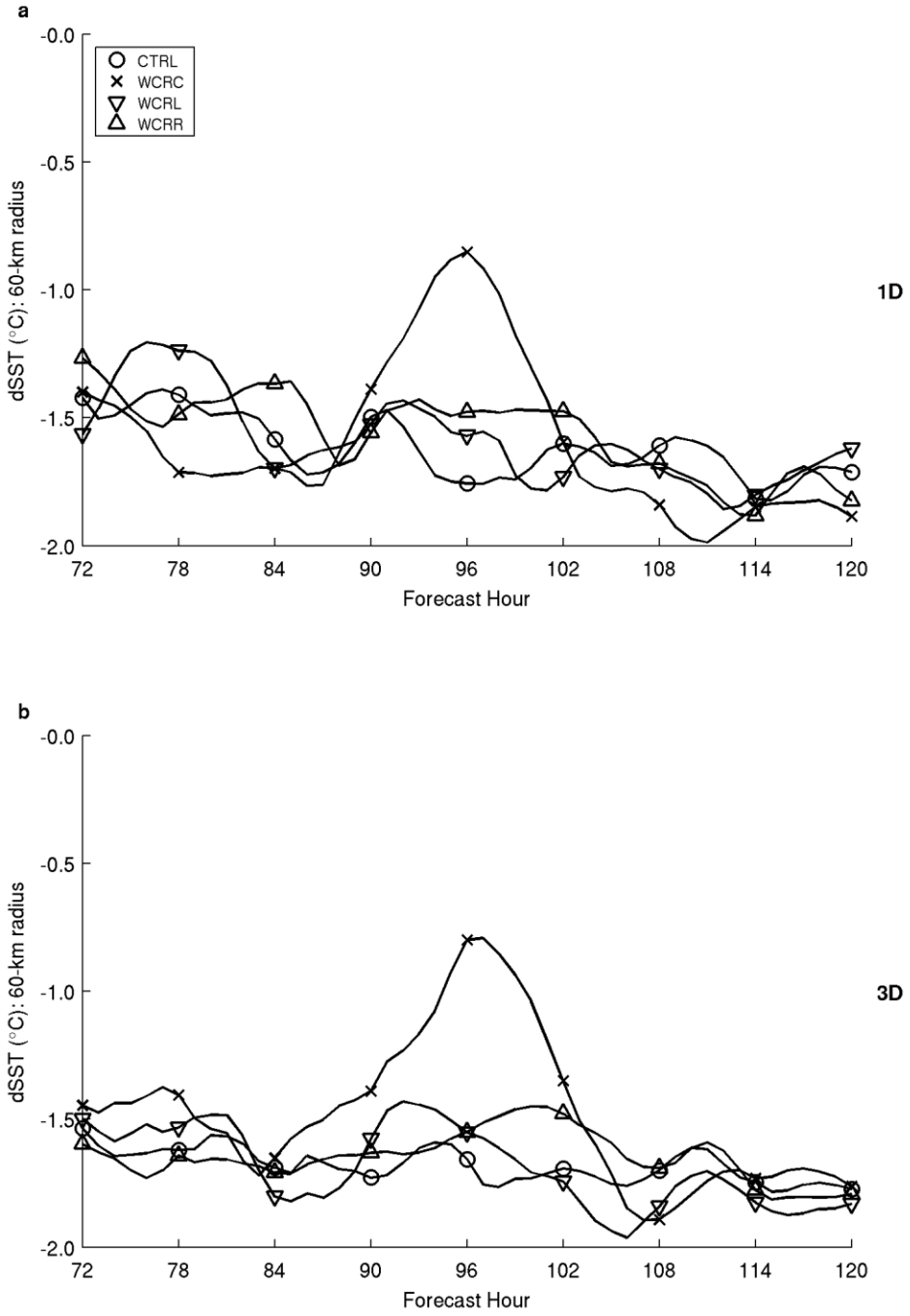

FIG. 7. Same as Fig. 5 but with an environmental wind speed of 5.0 m s^{-1}.

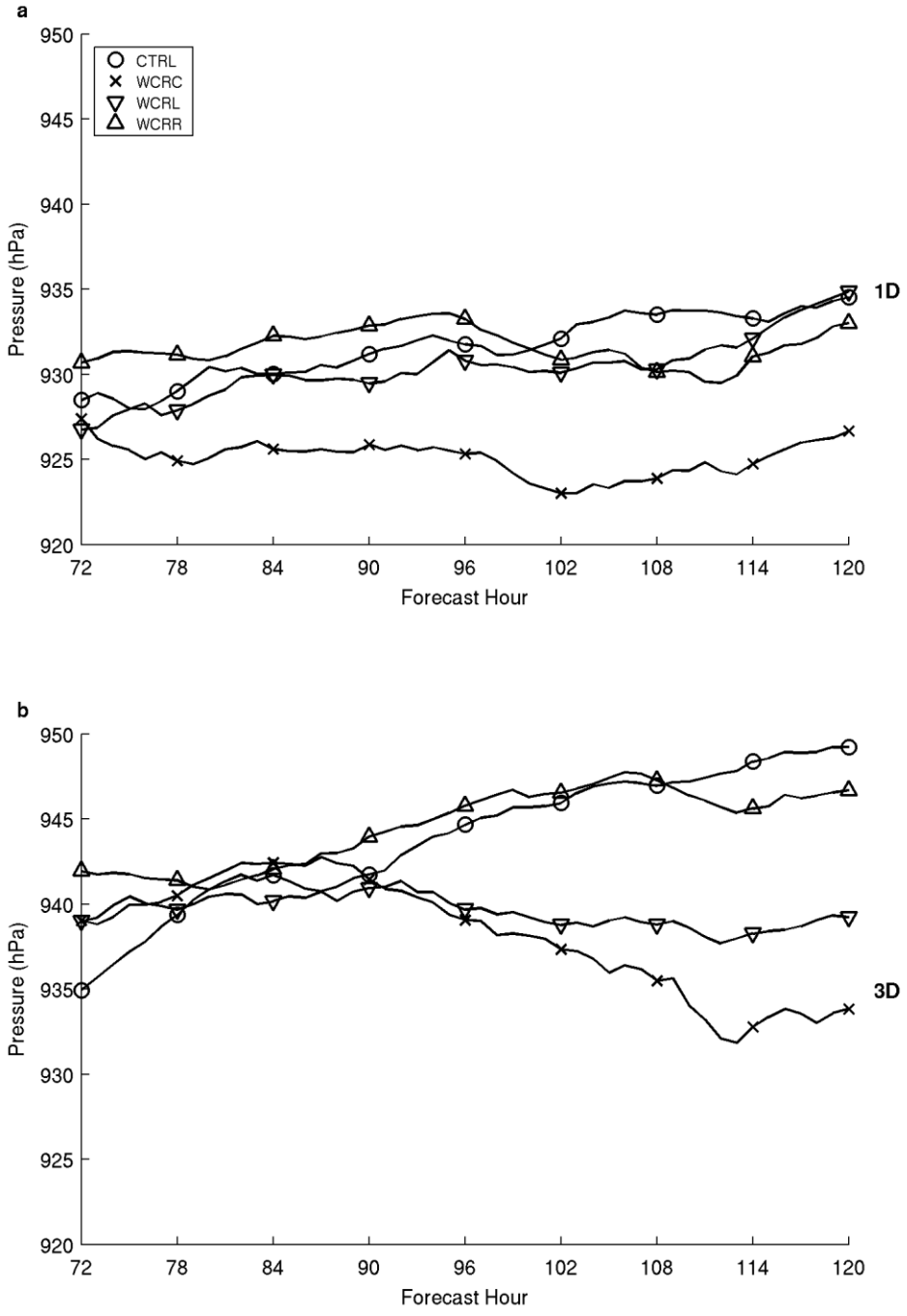

FIG. 8. Central pressure of the hurricane during hours 72-120 of the CTRL (“o”), WCRC (“x”), WCRL (downward triangle), and WCRR (upward triangle) coupled model simulations with an environmental wind speed of 0.0 m s^{-1} and ocean model dimensions of (a) 1D and (b) 3D.

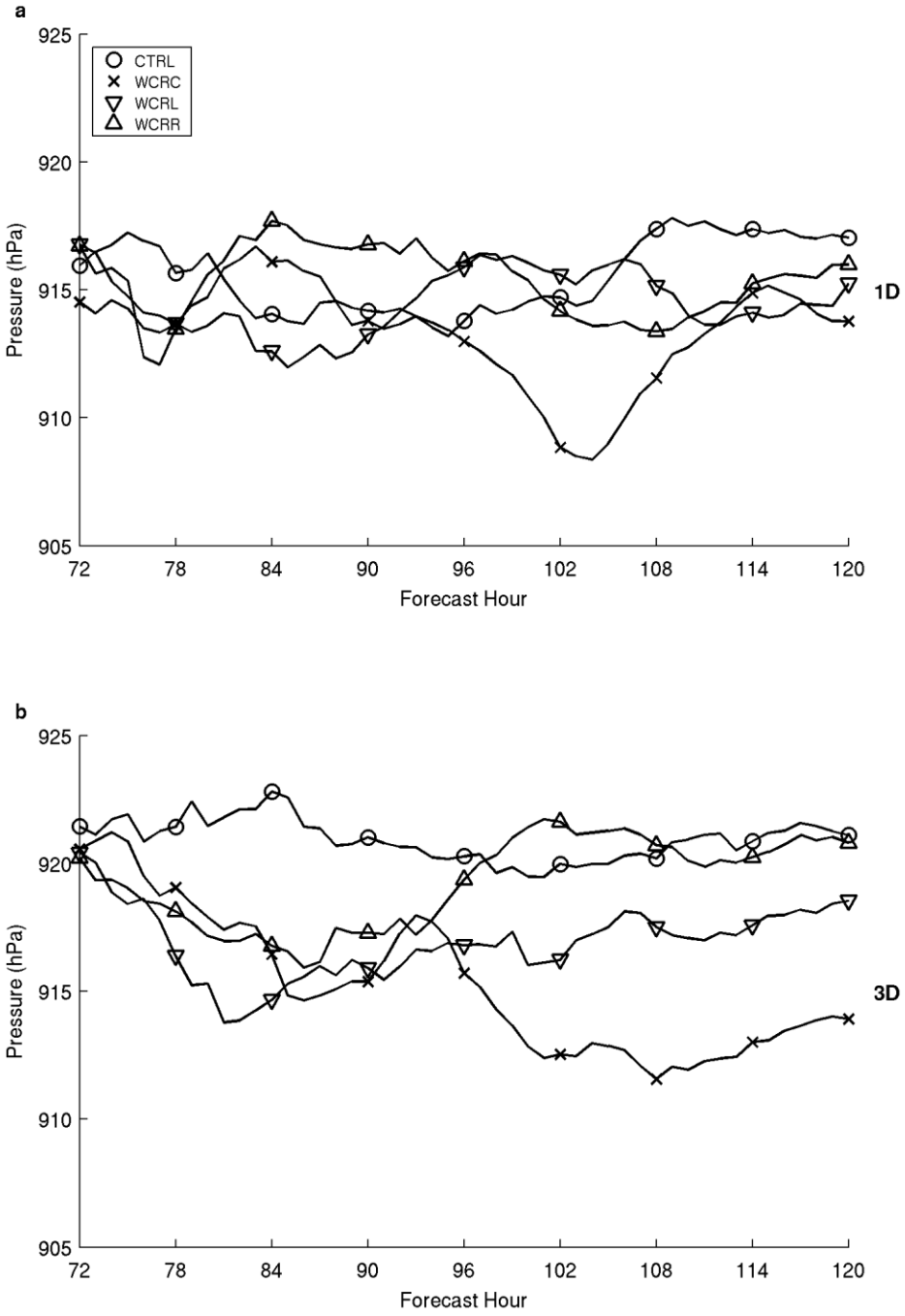

FIG. 9. Same as Fig. 8 but with an environmental wind speed of 2.5 m s^{-1}.

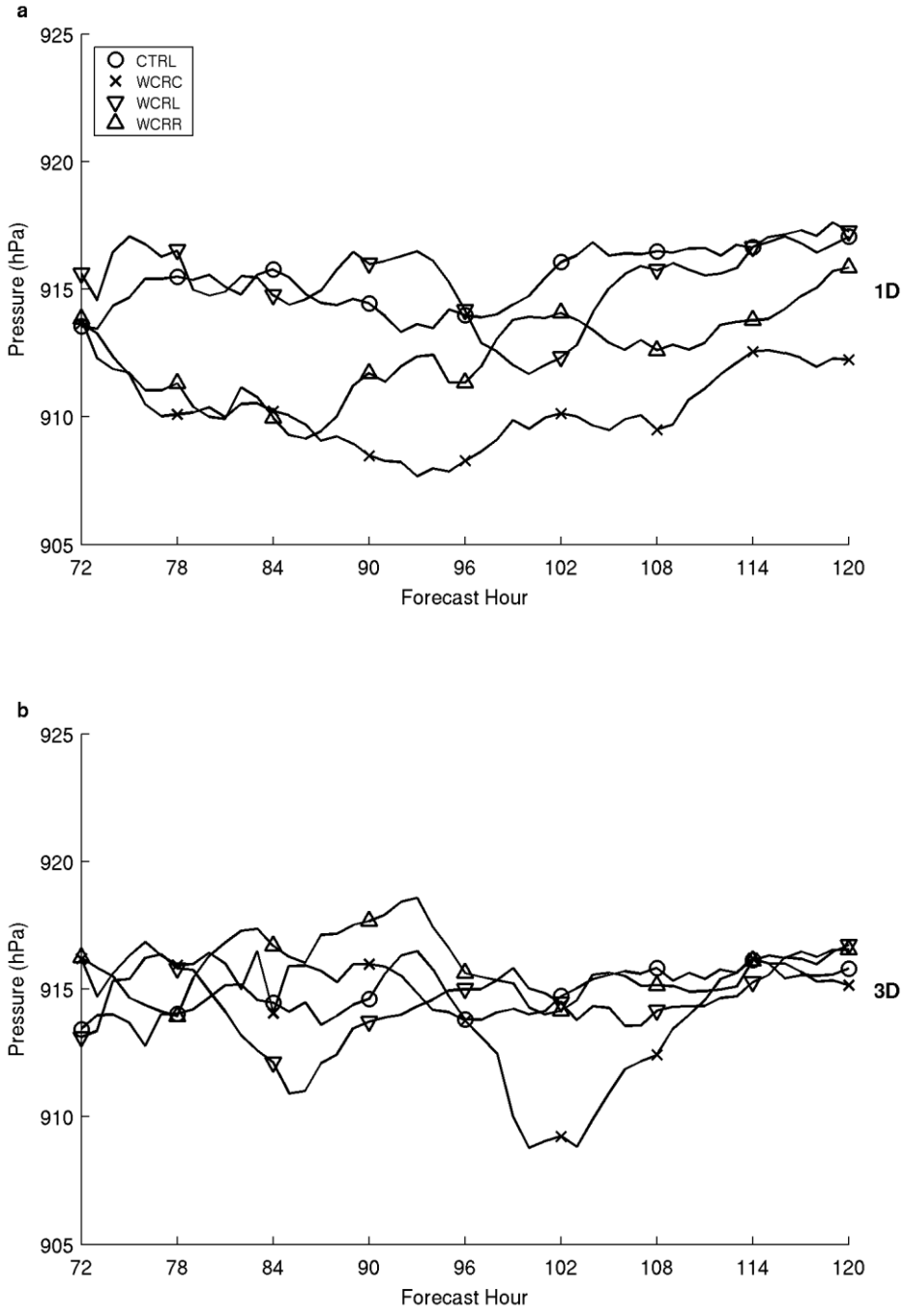

FIG. 10. Same as Fig. 8 but with an environmental wind speed of 5.0 m s^{-1}.